Biomed Microdevices (2013) 15:759–766
DOI 10.1007/s10544-013-9761-0

Fabrication of electro-microfluidic channel for single cell electroporation

Mehdi Shahini · Frans van Wijngaarden · John T. W. Yeow

Published online: 15 March 2013

Abstract The point of this paper is to demonstrate the use of a quick and cheap fabrication method to realize a laser-ablated microfluidic channel for single cell electroporation. Traditional lithography of microchannel with electrode in MEMS applications has always been complicated. Here, we introduce a new methodology of fabricating microchannel with electrical functionalities achieved through a fast and cheap process. In the present methodology, the microchannel pattern is cut out of polyimide, bonded to two ITO-coated substrates using Teflon as an adhesion layer. ITO as conductive material enables electric field in the channel and its optical transparency allows microscopy techniques to be utilized in characterizing the behavior of the microfluidic chip. The performance of the chip was tested on irreversible single-cell scale electroporation which requires relatively high voltages. CHO cells, as mammalian cells, were passed through the microchannel to experience electric field. Cells were loaded with a fluorogenic dye, Calcein AM, and the electroporation of each was individually recorded in real-time via fluorescent microscopy. The results show promising performance of the electric microchannel in electroporation. By customizing of ITO electrodes and the design of microchannel pattern, utilization and integration of the proposed electrical microchannel in variety of other MEMS-based devices are achievable.

Mehdi Shahini and Frans van Wijngaarden contributed equally.

M. Shahini · J. T. W. Yeow (✉)
Department of Systems Design Engineering,
University of Waterloo, Waterloo, Canada
e-mail: jyeow@uwaterloo.ca

F. van Wijngaarden
MESA + Institute for Nanotechnology,
University of Twente, Enschede,
The Netherlands

Keywords Microfluidic channel · Polyimide · Laser ablation · CHO cell · Electroporation · Cell lysis

1 Introduction

Microfluidic chips have been in use for well over a decade, and for a wide variety of applications. These range from the very basic early uses for ink jet printer heads to complicated micropumps and valves to be used in Lab-on-a-Chip (LOC) devices (Yoo et al. 2008). Recent developments have been mostly driven by these LOC possibilities, bringing advantages in healthcare, for example detection of malaria (Hou et al. 2010), analysis of single cells (Van den Brink et al. 2011) and lowering the cost of such systems (Govindarajan et al. 2012).

Most microfluidic devices are created as low-cost disposables, in order to minimize the risk of sample contamination and increase their usefulness in developing countries. For this application, polymers are very well suited, being cheap, easy to work with and available with a wide range of specifications (Becker and Gärtner 2008). Popular polymers for microfluidic applications are PMMA (Yoo et al. 2008), PDMS (L. Brown et al. 2006) and SU-8 (Abgrall et al. 2006). Polyimide is also often used for microfluidics (Metz et al. 2001), offering excellent properties specifically for biological applications, such as good thermal stability, low uptake of water and good biocompatibility. There are also no known solvents for polyimide (Becker and Gärtner 2008), giving it an excellent chemical stability. Its low absorption is especially advantageous when compared to the other popular polymer PDMS, which does suffer from such problems (Toepke and Beebe 2006). Fabrication methods used to create the microfluidic channels are mostly derived from the semiconductor industry, and include photolithography (Haraldsson et al. 2006),

etching (Oh 2008) and laser ablation (Yin et al. 2005). Laser ablation is most often performed using excimer laser systems (Kim and Xu 2003), operated at wavelengths from 193 nm to 355 nm. This technique provides good results and excellent controllability, allowing easy creation of new patterns for prototyping.

Often, electrodes are incorporated with microfluidic channels, allowing functions such as cell lysis (Lee and Cho 2007), electrochemical detection (Liu and Cui 2005), the manipulation of the liquid (Rajaraman et al. 2006) or simply as pads and wires for connecting the chip to external equipment.

Electroporation is the phenomenon in which pores are created across cell membrane as a result of exposure of cell to an external electric field. Variety of other mechanisms can be utilized for cell lysis (R. B. Brown and Audet 2008), with each technique having advantages and disadvantages compared to other techniques. Chemical lysis techniques are the most common lysis mechanism which has been widely implemented in LOC. However, chemical lysis techniques introduce chemicals to the lysate, which could require additional purification steps downstream depending on the intended application of a microfluidic LOC device. Electroporation does not have this disadvantage. No specific chemicals need to be added to the cell solution, and the lysate does not contain unwanted chemicals. The disadvantage of electrical poration of cells is that, in general, relatively high voltages and bulky power supplies are needed. Such techniques also require creation of electrodes in the microfluidic chip. Creation of such electrodes can be done in multiple ways; for example, by depositing thin (typically 50–250 nm) metal layers on the polymer in vacuum. However, since polymers have much greater thermal expansion coefficients, the temperature during deposition must be kept near room temperature to prevent cracking in the metal electrode layers. Another disadvantage is that lift-off lithography must be used to achieve features less than 10 μm in size, and most polymers are chemically incompatible with the photoresist and developer used in such steps. If a thick-film method is used, no vacuum is required. In such a method, a paste of metallic particles is smeared on a mask placed over the sample. The mask is then removed, and the residue left to dry. This typically yields electrode thicknesses of tens of micrometers, and worse resolution than shadow mask methods (Becker and Gärtner 2008). In contrast, glass slides coated with Indium Tin Oxide (ITO) can be easily used. If chip-wide electrodes are all that is required, no extra steps at all are required. If more intricate electrode patterns are required, lithography can be easily done on the chips, without suffering from the thermal expansion mismatch when depositing on polymers. Previously, transparent ITO substrates have been used in microfluidic applications (Yoo et al. 2008); (Kasahara et al. 2012), but never in combination with laser-ablated polyimide.

The laser ablation fabrication technique is well suited for fabricating microfluidic channels in polyimide. It is fast, detailed, controllable and very flexible. However, most laser systems used are excimer lasers, which are bulky and require sophisticated systems for handling the toxic gas used. In this paper, we present a method of ablating microfluidic channels in polyimide using a 30 W CO_2 laser with a wavelength λ=10.6 μm. Although lacking the resolution of excimer lasers, this system is low-cost, safe and easy to handle. Laser ablation using excimer lasers of polymers is a complicated process of both photothermal and photochemical breakup of the polymer chains (Shin et al. 2007). In contrast, the infrared wavelength of a CO_2 laser means that it always ablates the material photothermally. Although CO_2 laser ablation of polymers has been done before (Klank et al. 2002), it has not been done on polyimide. Bonding of polyimide can be performed in multiple ways, with lamination by far the most used method. When creating a polyimide-polyimide bond in this way, polyamic acid can be used as a solvent to enact diffusion of the polymer chains, yielding a very strong bond (Metz et al. 2001). This method has the disadvantage that it results in shrinkage of the polyimide, reducing the control over the feature size. On the other hand, using polyimide with a FEP coating (such as DuPont's Kapton™ Type FN), no additional solvents are needed, and bonding can be done by simple thermal lamination techniques.

In this work, we combine many of the easiest techniques to create a low-cost, quick and versatile method for prototyping microfluidic chips. Use of transparent ITO coated substrates will allow easy electrode creation, while retaining the ability to quickly image the channel performance using optical microscopy techniques. The use of a CO_2 laser will give great flexibility in channel design, without the difficulties normally associated with handling an excimer laser. This method has a low start-up cost, but the cost per unit does not decrease appreciably for larger volumes. Therefore, our method will be most useful for rapid prototyping and characterization of microfluidic chips, rather than bulk-volume fabrication.

2 Microchannel fabrication

Our microfluidic channels are made by using a 10.6 μm CO_2 laser engraving system (Universal Laser Systems, VLS2.30) to cut the channels completely through polyimide (DuPont Kapton FN 200FN919), thus yielding channels of the same height as the thickness of the polyimide layer.

Our tests on cutting 50-μm thick polyimide showed that engraving at 1 % of the maximum power (30 mW) and 1 %

of the maximum speed (0.25 mm/s), and making 3 passes over the same pattern yields the best results. At this speed, hardly any material is ejected from the channel, but rather is left behind as residue of broken monomers. This residue is easily removed after machining using ethanol as a cleaning agent. Engraving at higher power and/or speed caused an excess of heat buildup in the sample, resulting in thermal buckling and loss of positional control of the laser spot on the polyimide. Using the same laser, access holes to the microfluidic channels are drilled in the backside of the ITO-coated slides (Sigma Aldrich, 30–60 Ω/sq, Cat. No. 703184). The experimentally optimized settings for laser cutting/engraving of all components used for the microchannel are listed in Table 1. PMMA cutting and engraving were performed to provide the customized chip holders.

The polyimide used (Kapton FN) is pre-coated on both sides with Teflon FEP fluoropolymer as adhesive layers. This FEP coating can be bonded to ITO glass by heating it to 280 °C under pressure of a small vise, and letting it gradually cool. Samples of laser-cut polyimide before and after bonding are seen in Fig. 1. A sample line scan by a Dektac surface profilometer made perpendicular to the channel is illustrated in Fig. 1c. The roughness at the edges is diminished after bonding to ITO-coated cover slips. ITO-coated cover slips (SPI supplies, 30–60 Ω/sq, Cat. No. 06467-AB) was used in this sample. It should be noted that the ITO-coated cover slip, as thin as 130–170 μm, provides capability of imaging in higher magnifications where the microscope's objective lens has to be in such tiny distance to the specimen in the channel. Since CHO cells are big enough to be visible in lower magnifications, the chips used in this report are all made with ITO-coated glass slides.

The chip that is presented in this paper contains simple straight channels that are 3 mm in length. The width is 200 μm. The Kapton is cut to size using the laser cutter, and the channel is cut within it. The ITO-coated slides, having a sheet resistance of 30–60Ω/□, are also laser-drilled. All components are then cleaned using an ultrasonic cleaner (FisherScientific, FS30D), and are rinsed thoroughly by hand using ethanol. The whole stack is bonded in a vacuum oven, and syringe tips are attached and glued in place over the access holes in the bottom ITO-coated slide. For gluing, epoxy glue thickened with fumed silica is used. Normal epoxy glue was found to be not viscous enough, and was likely to flow into the microfluidic channels, thereby blocking them. During experiments, tubes will be attached to the syringe tips. The whole chip is then placed on a PMMA support structure, allowing top-down observation by fluorescence microscope while leaving room for the tubes to be guided away to syringes and waste disposal vials. A snapshot of the chip is depicted in Fig. 2.

3 Cell preparation

Chinese Hamster Ovary cell line CHO-K1 (ATCC, Cat. No. CCL-61) was used as a sample for mammalian cells. The frozen cells thawed in growth medium, containing F-12 Kaighns (Fisher Scientific, Cat. No. SH3052601) supplemented by 10 % Fetal Bovine Serum (Fisher Scientific, Cat. No. SH3039602) and 1 % Penicillin / Streptomycin (Bio Basic Canada, BS732). The cell medium transferred to a cell culture flask was incubated at 37 °C with 5 % CO_2. Every 2 days, cells were sub-cultured as follows: the cell medium was aspirated from cell culture flask and then, cells were washed by PBS. One milliliter of Trypsin 0.25 % (Fisher Scientific, Cat. No. SH3004202) was then added to the medium in order to detach cells. After 5 min incubation in room temperature, 7 ml of cell growth was added to the medium to stop detaching. Cells were transferred into a centrifuge tube and centrifuged in 2300 rpm for 1 min. The supernatant was discarded and electroporation buffer (10 mM phosphate buffer and 250 mM sucrose, pH 7.4) was replaced.

4 Cell electroporation

To show the useful and correct operation of our microfluidic chip, electroporation experiments have been done. In general, there are many different techniques for lysis or poration of cell membranes. Optical lysis (Rau et al. 2006) induces a bubble, and lyses cells by cavitation of that bubble. It is a fast technique, and therefore very useful for investigating processes within the cell requiring good temporal resolution. However, it is not suited for lysing many cells, and requires bulky equipment. Mechanical lysis uses surfaces with nano-scale barbs attached (Di Carlo et al. 2003). This method does not require bulky equipment during lysis, but carries the risk of blocking due to the generally low size of the channels compared to the cells. Increasing channel size greatly reduces lysis efficiency. Acoustic lysis also induces cavitating bubbles to lyse cells (Marmottant and Hilgenfeldt 2003). However, unlike optical lysis, acoustic lysis takes place over a relatively long time, and can significantly heat up the solution, resulting in denaturing of proteins inside the cell cytoplasm. Chemical lysis techniques are also well suited for bulk lysis, leading to high throughput (Listwan et al. 2010). However, chemical lysis techniques introduce chemicals to the lysate, which could require additional purification steps downstream, depending on the intended application of a microfluidic LOC device.

In electrical lysis of the cells, a voltage is applied across the cell solution. The resulting electrical field causes a voltage drop across the membrane (transmembrane potential), which introduces pores. If the transmembrane potential is large

Table 1 Laser settings used for different components of microchip

Material	Thickness (mm)	Power	Speed (mm/s)	Iterations
Kapton Polyimide	0.05	30 mW	0.25	3
ITO-coated microscope slide	1.1	1.5 W	0.5	10 times from each side
PMMA cutting	4.5	24 W	2.5	1
PMMA engraving	1.1	1.5 W	2.5	5

enough, and is maintained long enough, these pores can permanently disrupt the cell membrane thereby lysing it. The voltage applied to the chip (operational voltage) must be high enough to induce the required transmembrane potential. The following equation obtains the threshold value for external field for a spherical cell with the radius of a:

$$V = 1.5\,E_{ext}\,a\,\cos\theta\left(1 - e^{-t/\tau}\right) \quad (1)$$

where θ is the polar angle with respect to the direction of external field and τ is calculated from the following equation (Kinosita et al. 1988):

$$\tau = (\rho_1 + \rho_2/2)\,C\,a \quad (2)$$

In Eq. 2, ρ_1 and ρ_2 are the resistivities of cell medium and cytoplasm, respectively, and C is the capacitance of cellular membrane per unit area. These equations represent the fact that electroporation depends on the strength of electric field as well as the duration of time the field is applied. Since the threshold operational voltage is dependent on the system characteristics, the consequent external field (E_{ext}) applied

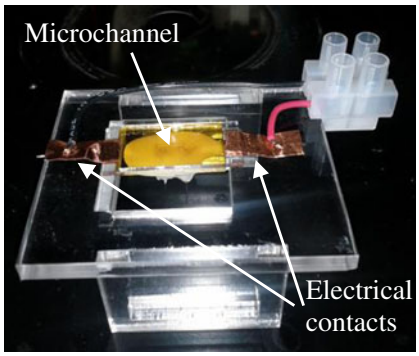

Fig. 2 snapshot of the fabricated electro-microfluidic chip for mammalian cell electroporation

to the cell-containing medium is more common in reports. The threshold values for electroporation of CHO cells have been studied by Valic et al. (Valic et al. 2003). They have reported the threshold strength of electric field within the range of 200–250 V/cm with pulses of milliseconds in duration. Electroporation can happen within 30 ms, if suitably high voltages and channel designs are used (Wang and Lu 2006a). Tweaking the pulse characteristics of a pulsed electrical field can also improve efficiency (Stroh et al. 2010). The difference between reversibly electroporating a cell and lysing a cell is mostly a matter of field strength and exposure time, both of which can easily be controlled.

Electroporation methods also do not introduce any chemicals to the lysate, thus eliminating the need for extra purification steps downstream in a LOC device. The disadvantage of electrical poration methods is that it requires electrodes to be specially added to the microfluidic chip

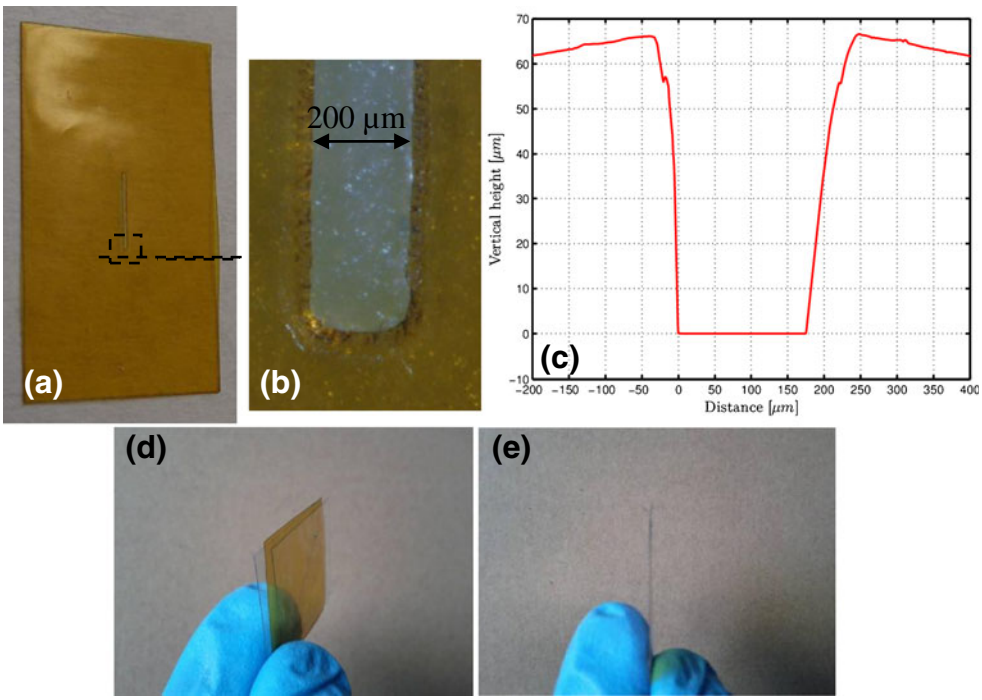

Fig. 1 Samples of laser-ablated poyimide, **a** post-cutting but pre-bonding, **b** under 11.25× magnification, **c** line scan made by a Dektac surface profilometer made perpendicular to the channel, **d** polyimide samples after bonding to ITO-coated cover slips, **e** front view of the bonded polyimide

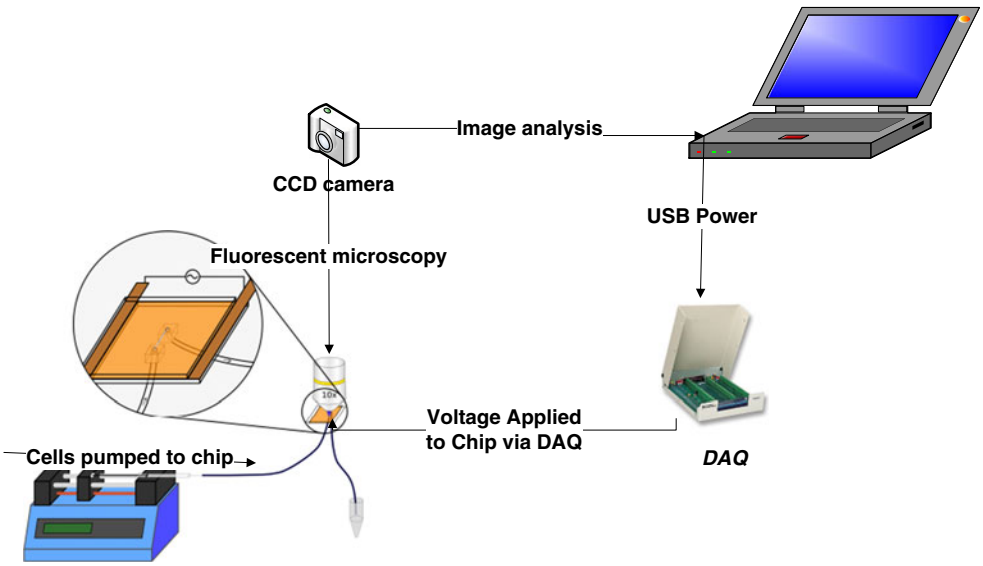

Fig. 3 Schematic overview of the experimental setup

for lysis, which complicates manufacturing. It also generally requires high voltages.

Reduction of electrode distance is the most common technique to diminish the high voltage requirements. Micro-distant electrodes have become more and more convenient to be created, due to developments in microfabrication techniques. Three-dimensional structure is one approach which requires more complicated fabrication compared to planar electrode system (H. Lu et al. 2005; K.-Y. Lu et al. 2006). However, low throughput of such systems still remains a big disadvantage since the channel size is limited by the capillar electrodes. In an attempt to remedy this, field enhancement via carbon nanotubes, taking advantage of the lightning rod effect, has been tried (Shahini and Yeow 2011). Recently, high-throughput microfluidic chips with 3D carbon electrodes have been developed (Mernier et al. 2012). Still, most of these techniques require rather extensive manufacturing steps. The fabrication process for microfluidic chips that we present in this paper lacks complicated 3D structures, but is made using a simple process without suffering from too severe limitations in throughput and voltage requirements.

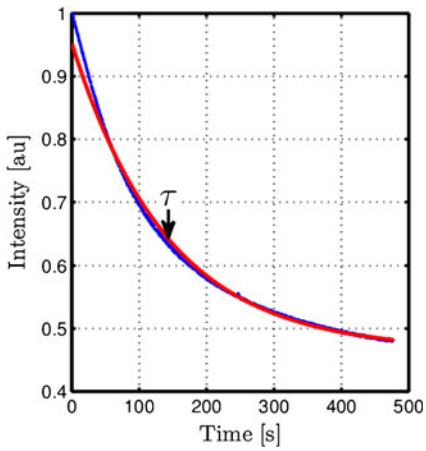

Fig. 4 Fluorescence decay of CHO cells loaded with Calcein-AM (*blue*) and the fitting exponential graph (*red*)

5 Results & discussion

Cell electroporation was performed as one example of the applications of the proposed polyimide-made electro-microfluidic channel. Direct imaging of lysis was used as a method to determine whether the microfluidic chip was capable of electroporating cells.

The prepared cells were loaded with Calcein-AM dye and imaged using fluorescent imaging. Calcein-AM is a non-fluorescent cell-permeable compound that hydrolyses to the fluorescent anion Calcein inside the cells. Before switching on the electrical field, the cells were very visible green dots. This allowed for following the cells in real-time during lysis. Cells were pumped to the chip through silicone tubing (VWR, Cat. No. CA62999-850). The pump turned off and cells became stationary before operational voltage was applied. A data acquisition system (DAQ) was used to supply operational pulse voltage and also to measure the passing current. Images were taken by a CCD camera (CoolSNAP, Turbo 1394 Series EZ) on a fluorescent microscope (Nikon Eclipse E600FN). Schematic view of the set-up of experiment is shown in Fig. 3

When a cell was electroporated, the fluorescent dye inside the cell would flow out through the ruptured membrane, and the brightness of the cell would reduce strongly. Electroporation is thus determined by watching the intensity of the fluorescent cell over time, and correlating this with the time the electrical field is switched on. The images were taken by the CCD camera at frame rate of 2 Hz with exposure time of 30 ms.

The Calcein AM dye did show deterioration when under prolonged excitation lighting, illustrated in Fig. 4, but this

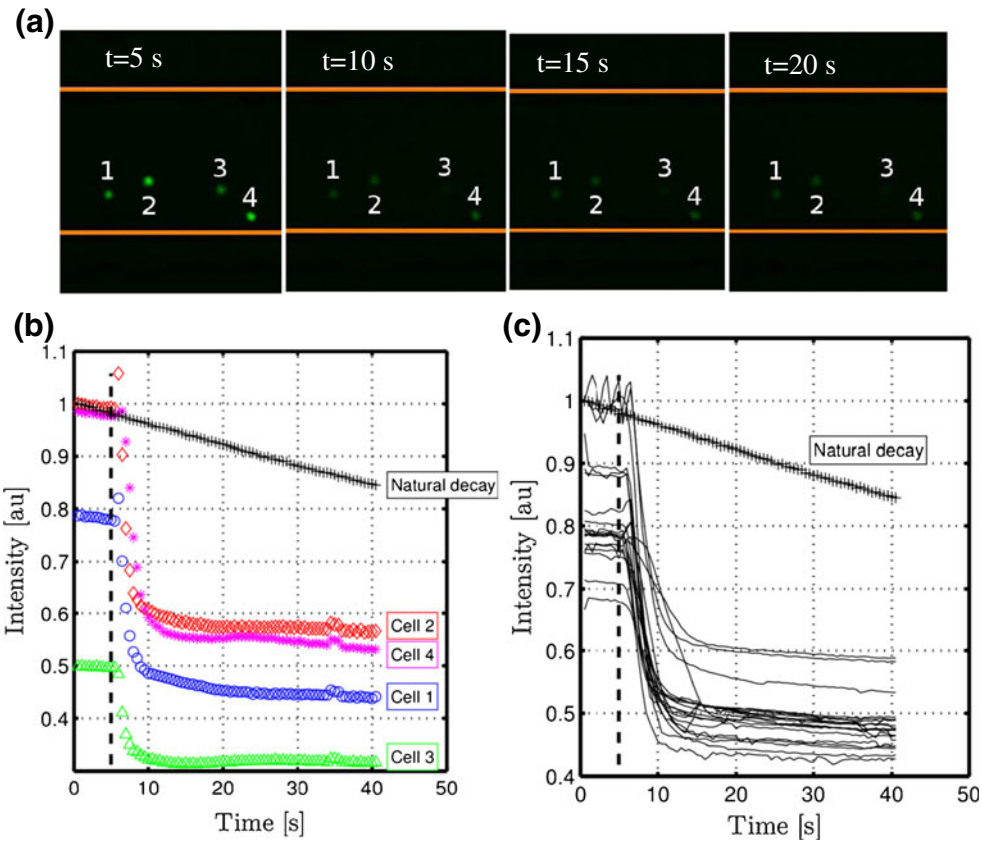

Fig. 5 Images of four cells loaded with Calcein AM dye, exposed to electric field at t=5 s and operational voltage of V=5 V (**a**). Total intensity of the square zones surrounding the four cells labeled in top image (**b**) and more cells experienced the same field (**c**)

process has a time scale of about 140 s. It is determined by fitting the normalized measured intensity graph with

$$I = I_0 \exp(-t/\tau) + I_{base}$$

where I_0 (= 0.4876) is the starting intensity, I_{base} (= 0.465) is the background intensity and τ (= 141.5 s) is the decay time constant. This deterioration is thus not significant when determining cell lysis through imaging, since that process takes place over a timescale of 10–20 s.

Figure 5a) shows images of four cells in the channel being electroporated within 20 s. The walls of the channel are depicted by orange lines in the pictures. The operational voltage of V=5 V was applied to the chip at the time of t=5 s. The drop in color intensity of Calcein-AM loaded cells indicates electroporation for all the four target cells.

The intensity of the cell spots in Fig. 5a is quantified by a MATLAB program and the results are shown in Fig. 5b. The intensity of all pixels in a square zone of 20×20 μm^2, surrounding each cell, is summed up and the total value is

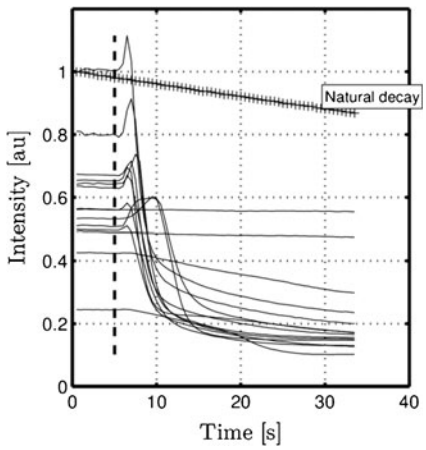

Fig. 6 Total intensity of the square zones surrounding individual cells, exposed to an electric field turned on at t=5 s with operational voltage of V=3 V

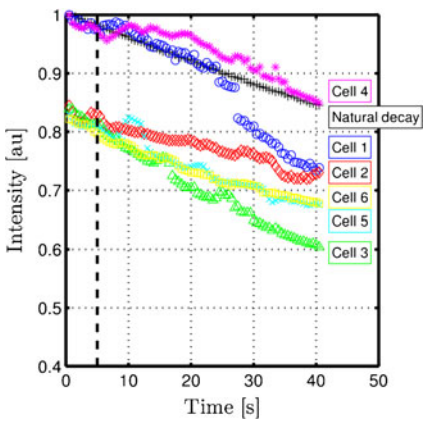

Fig. 7 Total intensity of the square zones surrounding individual cells, exposed to an electric field turned on at t=5 s with operational voltage of V=1 V

illustrated vs. time. The natural decay is also shown in the graph. The intensity of the brightest cell is normalized to start at 1, and the intensities of the other cells are normalized relative to the brightest cell using the ratio of maximum pixel values within the measured area. Even though the total intensities of the target cells are not equal at the time electric field is applied, the identical drops seen for the all cells indicate electroporation occurs within the first 5 s. It means the electric field in the channel is strong enough to electroporate cells with 100 % rate. The variation of the graph is not considerable after the time of t=10 s. To confirm that 100 % electroporation occurs at this voltage, more experiments have been performed at the same condition and the intensity variations of more cells are shown in Fig. 5c. The black dot line indicates the time electric field turned on.

The experiment was repeated with operational voltage of V=3 V. New chips were used to avoid contamination left from the previous experiments. The results for some target cells are illustrated in Fig. 6. As seen in the graph, nine cells out of thirteen are fully electroporated. An increase in the total intensity of the electroporated cell is visible right after electric field is turned on. It should be due to the abrupt expansion of the cell size while being electroporated (Bao et al. 2010; Wang and Lu 2006a, b)

The last experiment was performed at the operational voltage of V=1 V. As shown in Fig. 7, none of the target cells experienced full electroporation. It is understood that the strength of electric field is not high enough to affect membrane permeabilization of CHO cells.

The results presented here are samples to show the application of the electro-microchannel in electrical cell manipulation mechanisms. It is a promising approach to analyze behavior of single cells under electrical configurations. It should be noted that the capability of the proposed methodology is not limited to mammalian cells with relatively larger sizes. For electrical manipulation of smaller biosamples, for example bacteria, ITO-coated cover slip, as one sample is seen in Fig. 1, enables high magnification microscopic analysis. Moreover, the geometry customization of electrodes in deposition of ITO makes non-uniform eclectic fields in the microchannel. If such step is taken toward development of the chip, a broad range of cell treatments based on dielectrophoresis will be also achievable. Customized patterning of polyimide with no extra cost is another possibility toward integration and customization of the electro-fluidic channel in other on-chip cell manipulation systems.

6 Conclusion

In the present work, a cheap and fast fabrication methodology of making electric microchannel with Teflon-coated Kapton polyimide is presented. It is shown that a thin laser-ablated polyimide sheet thermally bonded to two ITO-coated glasses provides a cheap microchannel with electrical functionalities. The optical transparency and high throughput of the devices made by the methodology are the main features. Straight microchannels with 50 μm height were fabricated and their electrical performance was tested on irreversible electroporation of CHO cells. Different operational voltages (1–5 V) were applied to the chip and the fluorescent imaging of electroporation in real-time for individual cells was carried out. The results show a promising practicability of the proposed methodology in analysis of single cell electroporation. Further developments of the proposed electrical microchip by customizing ITO-coatings and polyimide cutting patterns are practical. Such developments will extend the application of the electrical microchip so that it can be utilized and integrated to many other MEMS devices.

Acknowledgement The authors thank Prof. Eijkel at University of Twente for his useful tips and suggestions and Prof. Pu Chen at University of Waterloo for providing us with CHO cells.

References

P. Abgrall, C. Lattes, V. Conédéra, X. Dollat, S. Colin, A.M. Gué, A novel fabrication method of flexible and monolithic 3D microfluidic structures using lamination of SU-8 films. J. Micromech. Microeng. **16**(1), 113–121 (2006). doi:10.1088/0960-1317/16/1/016

N. Bao, T.T. Le, J.-X. Cheng, C. Lu, Microfluidic electroporation of tumor and blood cells: observation of nucleus expansion and implications on selective analysis and purging of circulating tumor cells. Integr. Biol. **2**, 113–120 (2010). doi:10.1039/b919820b

H. Becker, C. Gärtner, Polymer microfabrication technologies for microfluidic systems. Anal. Bioanal. Chem. **390**(1), 89–111 (2008). doi:10.1007/s00216-007-1692-2

L. Brown, T. Koerner, J.H. Horton, R.D. Oleschuk, Fabrication and characterization of poly(methylmethacrylate) microfluidic devices bonded using surface modifications and solvents. Lab On A Chip **6**(1), 66–73 (2006). doi:10.1039/b512179e

R.B. Brown, J. Audet, Current techniques for single-cell lysis. J. Royal Soc., Interface / the Royal Society **5**(Suppl 2), S131–8 (2008). doi:10.1098/rsif.2008.0009.focus

D. Di Carlo, K.-H. Jeong, L.P. Lee, Reagentless mechanical cell lysis by nanoscale barbs in microchannels for sample preparation. Lab On A Chip **3**(4), 287–91 (2003). doi:10.1039/b305162e

A.V. Govindarajan, S. Ramachandran, G.D. Vigil, P. Yager, K.F. Böhringer, A low cost point-of-care viscous sample preparation device for molecular diagnosis in the developing world; an example of microfluidic origami. Lab On A chip **12**(1), 174–81 (2012). doi:10.1039/c1lc20622b

K.T. Haraldsson, J.B. Hutchison, R.P. Sebra, B.T. Good, K.S. Anseth, C.N. Bowman, 3D polymeric microfluidic device fabrication via contact liquid photolithographic polymerization (CLiPP). Sensors and Actuators B: Chemical **113**(1), 454–460 (2006). doi:10.1016/j.snb.2005.03.096

H.W. Hou, A.A.S. Bhagat, A.G.L. Chong, P. Mao, K.S.W. Tan, J. Han, C.T. Lim, Deformability based cell margination–a simple

microfluidic design for malaria-infected erythrocyte separation. Lab On A Chip **10**(19), 2605–13 (2010). doi:10.1039/c003873c

T. Kasahara, J. Mizuno, S. Hirata, T. Edura, S. Matsunami, C. Adachi, S. Shoji, *Microfluidic organic light emitting diode (OLED) using liquid organic semiconductors. 2012 IEEE 25th International Conference on Micro Electro Mechanical Systems (MEMS)*. (IEEE 2012), pp. 1069–1072. doi:10.1109/MEMSYS.2012.6170256

J. Kim, X. Xu, Excimer laser fabrication of polymer microfluidic devices, **15**(4), 255–260 (2003)

K. Kinosita, I. Ashikawa, N. Saita, H. Yoshimura, H. Itoh, K. Nagayama, A. Ikegami, Electroporation of cell membrane visualized under a pulsed-laser fluorescence microscope. Biophys. J. **53**(6), 1015–9 (1988). doi:10.1016/S0006-3495(88)83181-3

H. Klank, J.P. Kutter, O. Geschke, CO(2)-laser micromachining and back-end processing for rapid production of PMMA-based microfluidic systems. Lab On A Chip **2**(4), 242–6 (2002). doi:10.1039/b206409j

D.W. Lee, Y.-H. Cho, A continuous electrical cell lysis device using a low dc voltage for a cell transport and rupture. Sensors and Actuators B: Chemical **124**(1), 84–89 (2007). doi:10.1016/j.snb.2006.11.054

P. Listwan, J.-D. Pédelacq, M. Lockard, C. Bell, T.C. Terwilliger, G.S. Waldo, The optimization of *in vitro* high-throughput chemical lysis of Escherichia coli. Application to ACP domain of the polyketide synthase ppsC from Mycobacterium tuberculosis. J. Struct. Funct. Genomics **11**(1), 41–9 (2010). doi:10.1007/s10969-009-9077-8

C.C. Liu, D.F. Cui, Design and fabrication of poly(dimethylsiloxane) electrophoresis microchip with integrated electrodes. Microsyst. Technol. **11**(12), 1262–1266 (2005). doi:10.1007/s00542-005-0608-3

H. Lu, M.A. Schmidt, K.F. Jensen, A microfluidic electroporation device for cell lysis. Lab On A Chip **5**(1), 23–9 (2005). doi:10.1039/b406205a

K.-Y. Lu, A.M. Wo, Y.-J. Lo, K.-C. Chen, C.-M. Lin, C.-R. Yang, Three dimensional electrode array for cell lysis via electroporation. Biosens. Bioelectron. **22**(4), 568–74 (2006). doi:10.1016/j.bios.2006.08.009

P. Marmottant, S. Hilgenfeldt, Controlled vesicle deformation and lysis by single oscillating bubbles. 153–156 (2003). doi:10.1038/nature01592.

G. Mernier, R. Martinez-Duarte, R. Lehal, F. Radtke, P. Renaud, Very high throughput electrical cell lysis and extraction of intracellular compounds using 3D carbon electrodes in Lab-on-a-Chip devices. Micromachines **3**(3), 574–581 (2012). doi:10.3390/mi3030574

S. Metz, R. Holzer, P. Renaud, Polyimide-based microfluidic devices. Lab On A Chip **1**(1), 29–34 (2001). doi:10.1039/b103896f

S.R. Oh, Thick single-layer positive photoresist mold and poly(dimethylsiloxane) (PDMS) dry etching for the fabrication of a glass–PDMS–glass microfluidic device. J. Micromech. Microeng. **18**(11), 115025 (2008). doi:10.1088/0960-1317/18/11/115025

S. Rajaraman, H.M. Noh, P.J. Hesketh, D.S. Gottfried, Rapid, low cost microfabrication technologies toward realization of devices for dielectrophoretic manipulation of particles and nanowires. Sensors and Actuators B: Chemical **114**(1), 392–401 (2006). doi:10.1016/j.snb.2005.06.022

K.R. Rau, P.A. Quinto-Su, A.N. Hellman, V. Venugopalan, Pulsed laser microbeam-induced cell lysis: time-resolved imaging and analysis of hydrodynamic effects. Biophys. J. **91**(1), 317–29 (2006). doi:10.1529/biophysj.105.079921

M. Shahini, J.T.W. Yeow, Carbon nanotubes for voltage reduction and throughput enhancement of electrical cell lysis on a lab-on-a-chip. Nanotechnology **22**(32), 325705 (2011). doi:10.1088/0957-4484/22/32/325705

B.S. Shin, J.Y. Oh, H. Sohn, Theoretical and experimental investigations into laser ablation of polyimide and copper films with 355-nm Nd:YVO4 laser. J. Mater. Process. Technol. **187–188**, 260–263 (2007). doi:10.1016/j.jmatprotec.2006.11.106

T. Stroh, U. Erben, A.A. Kühl, M. Zeitz, B. Siegmund, Combined pulse electroporation–a novel strategy for highly efficient transfection of human and mouse cells. PLoS One **5**(3), e9488 (2010). doi:10.1371/journal.pone.0009488

M.W. Toepke, D.J. Beebe, PDMS absorption of small molecules and consequences in microfluidic applications. Lab On A Chip **6**(12), 1484–6 (2006). doi:10.1039/b612140c

B. Valic, M. Golzio, M. Pavlin, A. Schatz, C. Faurie, B. Gabriel, J. Teissié et al., Effect of electric field induced transmembrane potential on spheroidal cells: theory and experiment. European Biophysics Journal: EBJ **32**(6), 519–28 (2003). doi:10.1007/s00249-003-0296-9

F.T.G. Van den Brink, E. Gool, J.-P. Frimat, J. Bomer, A. Van den Berg, S. Le Gac, Parallel single-cell analysis microfluidic platform. Electrophoresis **32**(22), 3094–100 (2011). doi:10.1002/elps.201100413

H. Wang, C. Lu, Electroporation of mammalian cells in a microfluidic channel with geometric variation. Anal. Chem. **78**(14), 5158–64 (2006a). doi:10.1021/ac060733n

H. Wang, C. Lu, High-throughput and real-time study of single cell electroporation using microfluidics: effects of medium osmolarity. Biotechnol. Bioeng. **95**(6), 1116–1125 (2006b). doi:10.1002/bit

H. Yin, K. Killeen, R. Brennen, D. Sobek, M. Werlich, T. Van de Goor, Microfluidic chip for peptide analysis with an integrated HPLC column, sample enrichment column, and nanoelectrospray tip. Anal. Chem. **77**(2), 527–533 (2005). doi:10.1021/ac049068d

J.-C. Yoo, G.-S. La, C.J. Kang, Y.-S. Kim, Microfabricated polydimethylsiloxane microfluidic system including micropump and microvalve for integrated biosensor. Curr. Appl. Phys. **8**(6), 692–695 (2008). doi:10.1016/j.cap.2007.04.050